ISSN 1996-3343

Asian Journal of Applied Sciences

Knowledgia SCIENTIFIC
A Place to Publish Outstanding Research

http://knowledgiascientific.com

Asian Journal of Applied Sciences 1 (3): 185-205, 2008
ISSN 1996-3343

Analysis of Semi-Continuous Composite Beams with Partial Shear Connection Using 2-D Finite Element Approach

[1]Messaoud Titoum, [2]Mohamed Tehami, [1]Belkacem Achour and [3]Jean-Pierre Jaspart
[1]Department of Civil Engineering, Mostaganem University, Algeria
[2]Department of Civil Engineering, UST Oran, Algeria
[3]Department of Material Mechanics and Structures, Liège University, Belgium

Abstract: In this study, a two-dimensional finite element model using ANSYS software was proposed to study the behaviour of semi-continuous composite beams allowing for the concept of partial shear connection in both sagging and hogging moment regions. Some comparisons with experimental data available in the literature were reported to validate the efficiency of the proposed model. Using the verified model, a parametric study was carried out to investigate the effects of partial shear connection, along with the effects of reinforcing ratio and the presence of column web stiffeners, on the behaviour of semi-continuous composite beams. Based on the results obtained from the finite element analysis, the concept of partial shear connection in the hogging moment regions can be accepted provided that the shear connectors are sufficiently ductile, in spite of the requirement of full shear connection specified in Eurocode 4 for continuous and semi-continuous composite beams.

Key words: Composite beam, partial shear connection, composite joint, finite element method, ANSYS

INTRODUCTION

When composite beams in multi-storey buildings are attached to columns by semi-rigid and partial strength joints they are considered as semi-continuous. This new type of composite beams was adopted by the Eurocode 4 (1992) under the condition that full shear connection in the hogging moment regions is assured. Nevertheless, the results of the tests conducted by Aribert and Lachal (1992), Bode *et al*. (1997), Diedricks *et al*. (1999) and Loh *et al*. (2004, 2006) on composite beams and on composite joints showed the possibility of providing partial shear connection in the hogging moment regions of semi-continuous composite beams.

Many research works have been carried out to study the effects of partial shear connection in the case of simply supported composite beams. However, the effects of this parameter have not yet been clarified in the case of continuous and semi continuous composite beams. This situation has required the investigation of the issue of partial shear connection in the hogging moment regions by numerical procedures using the finite element method instead of experimental tests because of their set up complexity.

Since the beginning of the eighties, the finite element modelling of composite beams and composite joints started specially dealing with the problem of relative slip that always exists even with complete shear connection between the steel beam and the concrete stab as the shear connectors are rarely stiff enough to prevent all slip at the interface.

One-dimensional models developed by Aribert *et al*. (1993), Kattner and Crisinel (2000) and Dissanayake *et al*. (2000) gave satisfactory results for the global behaviour, but failed to provide results regarding the local responses, such as the distribution of stresses and strains over the entire section of

Corresponding Author: Messaoud Titoum, Department of Civil Engineering, Mostaganem University, Algeria
Tel: +213 45 23 27 12 Fax: +213 45 21 10 18

the structural components. However, two and three-dimensional models can simulate complex structures and can provide a wide range of results and all details of the behaviour. A summary of 2D and 3D models is showed in Table 1 and 2 for composite beams and for composite joints, respectively.

Table 1: 2D and 3D finite element models of composite beams

Authors (date)	FE model-software	Finite element types	Investigation
Hirst and Yeo (1980)	2D-standard finite element program	Eight-node isoparametric plane stress elements for both concrete slab and steel beam Quadrilateral plan stress elements for stud shear connectors	Analysis of composite beams using standard finite element programs
Razaqpur and Nofal (1989)	3D-developed program NONLACS	Four-node layered shell elements for concrete slab and flanges of steel beam Four-node quadrilateral plane stress elements for web of steel beam Three dimensional bar elements for shear connectors	Proposition of three dimensional bar element for modelling the nonlinear behaviour of shear connectors in composite beams
Sebastian and McConnel (2000)	3D-developed program	Four-node layered thin plate bending-membrane elements for concrete slab and smeared reinforcement Two-node layered bending-membrane elements for steel beam Stub elements for shear connectors	Development of a non-linear finite element program for the analysis of steel-concrete composite structures
Bascar *et al.* (2002)	3D-ABAQUS	Twenty-node solid elements for concrete slab Eight-node shell elements for steel beam Two-node beam elements for shear connectors	Finite element analysis of steel-concrete composite plate girder
Liang *et al.* (2004)	3D-ABAQUS	Four-node layered shell elements for concrete slab and smeared reinforcement Four-node shell elements for flanges and web of steel beam Two-node beam elements for stud shear connectors	Interaction strengths of continuous composite beams in combined bending and shear
Nie *et al.* (2004)	3D-ANSYS	Eight-node solid elements for concrete slab Four-node shell elements for flanges and web of steel beam Three dimensional bar elements for reinforcement bars Two dimensional linear spring elements for bond-slip relationship between concrete and reinforcement Two dimensional nonlinear spring elements for stud shear connectors	Stiffness of composite beams in negative bending regions by considering slips at the steel beam-concrete slab interface and concrete-reinforcement interface
Bujnak and Bouchair (2005)	3D-CASTEM 2000	Four-node layered shell elements for concrete slab and smeared reinforcement Four-node shell elements for flanges and web of steel beam Two-node beam elements for shear connectors	Finite Element Modelling of composite beams with partial shear connection
Queiroz *et al.* (2007)	3D-ANSYS	Eight-node solid elements for concrete slab with smeared reinforcement bars Four-node shell elements for flanges and web of steel beam Two dimensional nonlinear spring elements for shear connectors	Finite Element Modelling of simply supported composite beams with full and partial shear connection

NB: All the models took into account the nonlinear behaviour of concrete, structural steel, reinforcement bars and shear connectors

Table 2: 2D and 3D finite element models of composite joints

Authors (date)	FE model-software	Finite element types	Investigation
Lee and Lu (1991)	2D-ADINA	Quadrilateral and triangular plan stress elements for concrete slab, steel beam and steel column Two dimensional bar elements for reinforcement bars Elasto-plastic bar elements for stud shear connectors	Cyclic load analysis of composite connection sub-assemblages-effects of the composite action both in the slab and in the column web panel zone
Ebato *et al.* (1995)	3D-ANSYS	Eight-node solid elements for concrete slab Four-node shell elements for steel beam and steel column Three dimensional bar elements for reinforcement bars Two dimensional elasto-plastic spring elements for shear connectors	Finite element analysis of semi-rigid composite joints under non-symmetrical loading
Bursi and Caldara (1999)	3D-ABAQUS	Shell elements for concrete slab, steel beam and steel column Bar elements for reinforcement bars Non-linear spring elements for bond-slip relationship between concrete and reinforcement Non-linear spring elements for shear connectors	Non linear finite element study of steel-concrete composite sub structures with partial shear connection
Doneaux (2003)	3D-CASTEM 2000	Four-node layered shell elements for concrete slab and smeared reinforcement Four-node shell elements for steel beam and steel column Beam elements for shear connectors	Parametric study of the behaviour of composite beams in joints to exterior columns
Bursi *et al.* (2005)	3D-ABAQUS	Shell elements for concrete slab, steel beam and steel column Beam elements for reinforcement bars Non-linear spring elements for bond-slip between concrete and reinforcing bars Non-linear spring elements for shear connectors Linear truss elements to reproduce uplift	Investigation of the seismic performance of composite moment resisting frames with full and partial shear connection subjected to seismic loading
Salvatore *et al.* (2005)	3D-ABAQUS + ADINA	Eight-node and four-node solid elements for concrete slab, steel beam and steel column Beam elements for reinforcing bars Nonlinear spring elements for bond-slip between concrete and reinforcing Nonlinear spring elements for shear connectors in extension and shear	Investigation of the seismic performance of exterior and interior partial-strength beam to column joints
Fu *et al.* (2007)	3D-ABAQUS	Eight-node solid elements were used for all components of the connection: concrete slab, steel beam, steel column, reinforcing bars, stud shear connectors, end-plate and bolts Node-to-node contact elements for contact between the end-plate, column flange and bolt head	Parametric study of semi-rigid composite connections with steel beams and precast hollow core slabs

NB: All the models took into account the nonlinear behaviour of concrete, structural steel, reinforcement bars and shear connectors

Due to the complexity of three-dimensional models (meshing difficulties, memory requirements, numerical convergence problems and result interpretation difficulties), a two-dimensional model is then chosen for this study. In this study, the effects of partial shear connection on the behaviour of semi-continuous beams are investigated using ANSYS software (version 10). To validate the accuracy and

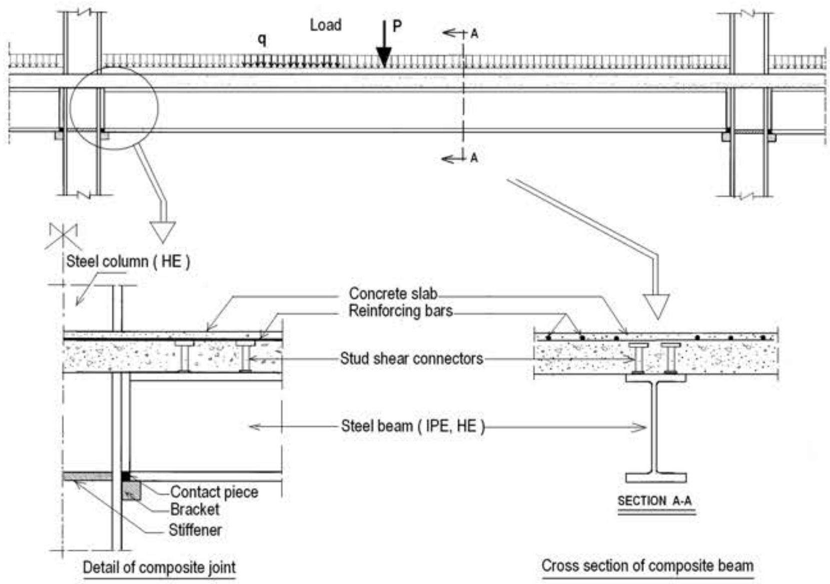

Fig. 1: System of semi-continuous composite beam in braced frame

efficiency of the proposed model, the numerical results were verified against test results available in the literature. A parametric study was performed to investigate the effects of partial shear connection, along with the effects of reinforcing ratio and the presence of column web stiffeners on the behaviour of semi-continuous composite beams.

Semi-Continuous Composite Beam System

The semi-continuous composite beam considered is shown in Fig. 1. Its ends are attached to the steel columns by means of semi-rigid and partial-strength composite joints. It is subjected to uniformly distributed and point loads, which generally occur in buildings.

The composite beam consists of an IPE profile, connected to the concrete slab by means of stud shear connectors welded on the top flange of the steel beam and embedded in the concrete slab.

The composite joint is characterised by the absence of bolts. The steel beam is connected to the steel column just using a contact piece and installed on a support plate (bracket) welded to the column flange. In this way the connection at the steel profile level is able to bear only shear forces without any moment transfer capacity; only the presence of longitudinal reinforcing bars through the column can lead the joint to bear bending moments (Fabbrocino *et al*., 2002). Moreover the columns are stiffened with transverse stiffeners welded to the web at the bottom beam flange level to avoid local buckling.

Finite Element Model

The system of semi-continuous composite beam shown in Fig. 1 was simulated by a two-dimensional finite element model using ANSYS software (version 10). The main components of this structure are: concrete slab, steel beam, steel column, reinforcing bars, shear connectors, contact piece, bracket and stiffeners. In order to obtain accurate results from the finite element analysis, all components must be properly modelled tacking into account their material nonlinearity. The deflections are assumed to be small relative to the main structural dimensions, therefore nonlinear geometric effects are not considered.

Finite Element Types

The finite element types considered in the model are as fallows:

- The concrete slab, steel beam, steel column, contact piece, bracket and stiffener were modelled using quadrilateral plane stress elements called PLANE42. The thicknesses of the plane stress elements assigned are equal to the effective widths of the concrete slab corresponding to the sagging or hogging moment region defined by Eurocode 4 (1992) as well as flange widths and web thicknesses of the steel sections as appropriate.
- The longitudinal reinforcing bars were modelled in a discrete manner using the two-dimensional spar element LINK1. In this study, full bond action was assumed because the bond-slip between the longitudinal reinforcing bars and concrete has little effect due to the presence of transverse reinforcing bars used to prevent longitudinal cracks caused by splitting and shear actions. Therefore, the nodes of LINK1 elements are attached to coincident nodes of PLANE42 elements of the concrete slab, so the two materials share the same nodes.
- The shear connectors were modelled using nonlinear spring elements COMBINE39 in their actual locations.
- The transfer of stress from the concrete slab to the top flange of the steel beam can be achieved by coupling every pair of coincident nodes at the interface. This arrangement allows slip but prevents overlapping or uplifting.

Finite Element Meshing and Boundary Conditions

The finite element meshing of the semi-continuous composite beam system is shown in Fig. 2. Symmetry considerations led to modelling only one half of the structure including some of the boundary conditions:

- All the nodes along the middle of the composite beam are restricted from moving in the X direction due to symmetry.
- All the nodes of the column axis are restricted from moving in X direction due to symmetry.
- The bottom ends of the column flange and web are restricted from moving in X and Y directions.
- The interface of composite beam is initially of zero length, but is shown in Fig. 2 to be of finite length (gap) for clarity.

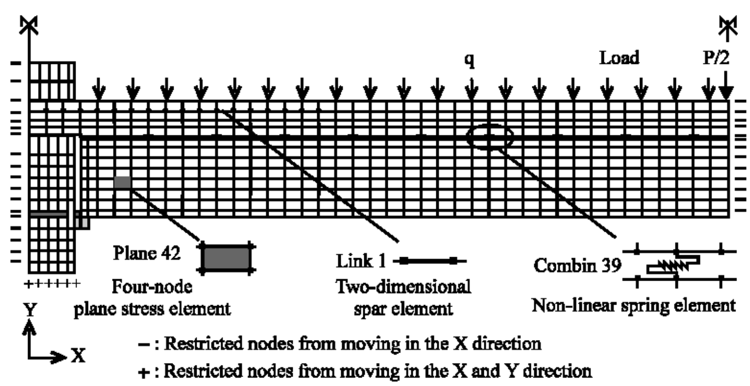

Fig. 2: Meshing and boundary conditions

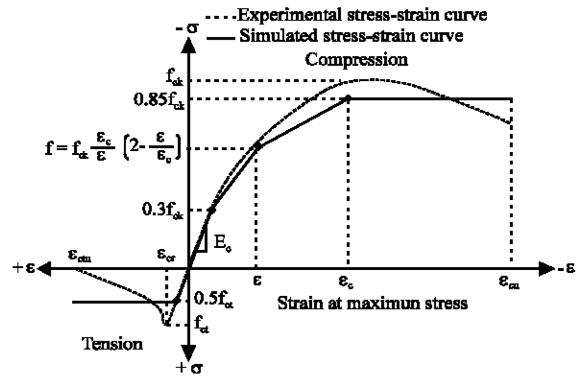

Fig. 3: Experimental and simulated stress-strain curves of concrete

Material Modelling of Concrete Slab

Concrete is a quasi-brittle material and has different behaviour in compression and tension. The tensile strength of concrete is approximately 10% of the compressive strength. Figure 3 shows an experimental stress-strain curve of normal weight concrete. In compression, the stress-strain curve is linearly elastic up to about 30% of the maximum compressive strength. After it reaches the maximum compressive strength f_{ck}, the curve descends into a softening region and eventually crushing failure occurs at an ultimate strain ε_{cu}. In tension, the stress-strain curve is approximately linearly elastic up to the maximum tensile strength f_{ct}. After this point, the concrete cracks and the strength decreases gradually to zero (Studer, 1985; Bangash, 1989).

A simplified material model having different properties in tension and compression was adopted here to simulate the concrete slab (Fig. 3). The stress-strain curve of concrete in compression is modelled by a multi-linear elastic-plastic law, while an elastic-perfectly plastic law models the concrete in tension assuming that this latter is also able to transfer tension after the formation of cracks. Hence, the softening branch remains horizontal up to failure.

The compressive and tensile regions must be identified since the ANSYS software cannot handle the two behaviours at the same time using plane stress elements. The hogging moment region, according to Eurocode 4 (1992), was found to span 15% of the composite beam length on each side of the supports.

Test results show also that, in the hogging moment regions, the concrete slab is mainly under tension except for the areas around the front of the stud shear connectors as shown in Fig. 4 where the concrete is in compression. Through this compression, the longitudinal shear force is transferred between the stud shear connectors and the longitudinal reinforcing bars (Fu *et al*., 2007).

- The strain at which maximum compressive stress occurs was taken as 0.0025, while the strain at which the concrete crushes, was taken as 0.0040.
- The concrete elastic modulus was evaluated according to Eurocode 4 (1992), by the following relation:

$$E_c = 9500\,(f_{ck}+8)^{1/3} \quad (1)$$

Material Modelling of Structural Steel and Reinforcing Bars

The structural steel and steel of reinforcing bars were modelled as an isotropic elasto-plastic material in both tension and compression taking into account hardening effects, giving a bilinear stress-

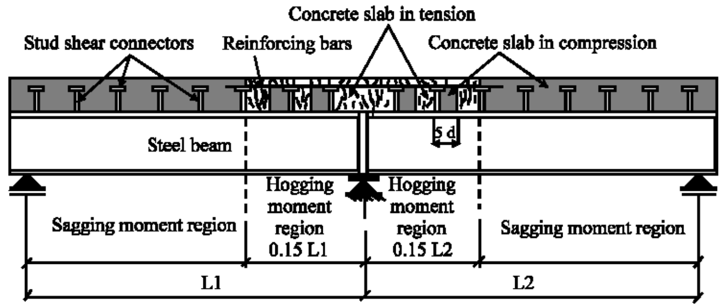

Fig. 4: Identification of compressive and tension areas

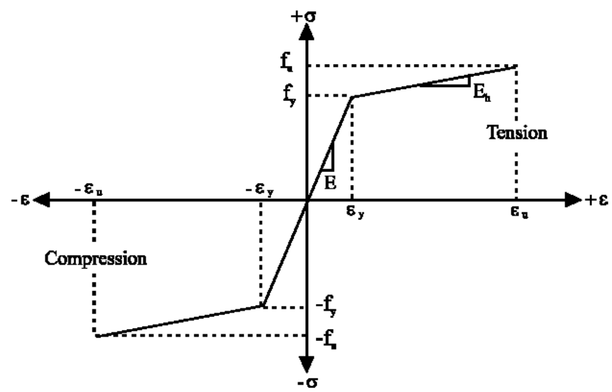

Fig. 5: Bilinear stress-strain curve of structural steel and reinforcing bars

stain relationship as shown in Fig. 5. This model was chosen because of its relative simplicity. The values of the following parameters E, v, f_y, f_u, E_h and ε_u which are respectively, the Young's modulus, the Poisson's ratio, the yield stress, the ultimate stress, the strain-hardening modulus and the ultimate strain, were needed to define this material model.

Modelling of Shear Connectors

The behaviour of a shear connector is generally defined by a nonlinear load-slip relationship, obtained from Push-Out tests. For stud shear connectors, this relationship can be modelled using the exponential function proposed by Ollgaard *et al*. (1971) as follows:

$$P\,(S) = Pu\,(1 - e^{-\beta|s|})\alpha \tag{2}$$

Where:

P (S)	=	Shear force on a stud shear connector
s	=	The value of the relative slip
α and β	=	Shape of the curve
P_u	=	Ultimate shear resistance of stud shear connectors, which can be determined by the following equation given by Eurocode 4 (1992):

$$P_u = \min\left[0.8f_u\left(\pi d^2/4\right)\;;\;0.29d^2\sqrt{f_{ck}E_{cm}}\right] \tag{3}$$

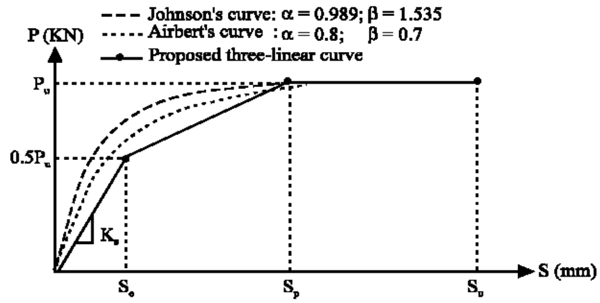

Fig. 6: Idealized load-slip curves of stud shear connector

Where:

f_u = The ultimate tensile strength of stud steel
d = The diameter of stud
f_{ck} = The compressive strength of concrete
E_{cm} = The elastic modulus of concrete

For the simplification of the numerical analysis, a tri-linear function of the load-slip curve, as shown in Fig. 6, was used rather than the exponential curve of Aribert and Labib (1982) or Johnson and Molenstra (1991).

- The initial shear stiffness K_{si} of stud shear connector can be determined by the following empirical equation proposed by Oehlers and Coughlan (1986):

$$K_{si} = \frac{P_u}{d(0.16 - 0.0017f_{ck})} \tag{4}$$

- The elastic slip S_e at the applied load of 0.50 P_u can be determined by the following equation:

$$S_e = \frac{0.50P_u}{K_{si}} \tag{5}$$

- For plastic slip S_p, the following equation was suggested

$$S_p = \frac{2 \cdot P_u}{K_{si}} \tag{6}$$

The ultimate slip capacity S_u, which represents the ductility of stud shear connector can be calculated, for the range of concrete cylinder strength, f_{ck} between 20 and 40 N mm^{-2}, by the empirical equation suggested by Johnson and Molenstra (1991) as follows:

$$S_u = (0.453 - 0.0018f_{ck}) \cdot d \tag{7}$$

Application of Loads

The load was incrementally applied to the model. The ANSYS software used the Newton-Raphson equilibrium iteractions to provide convergence at the end of each load increment within tolerance limits. In this study, convergence criteria were based on force and displacement and the convergence tolerance limits were initially selected by the ANSYS software. The convergence limits for this analysis used the L2-norm of force tolerance equal to 0.1% and an L2-norm check on displacement with 5% tolerance.

Failure Criterion

The failure of the semi-continuous composite beam may occur due to the following causes:

- Crushing of concrete in compression, which was assumed to occur at the ultimate strain ε_{cu}
- Fracture of structural steel, taken as when the ultimate strain ε_{au} was reached
- Cracking of concrete and fracture of longitudinal reinforcing bars in tension at the ultimate strain ε_{su}
- Failure of shear connectors due to excessive slip, taken as the ultimate slip S_u
- The failure due to local bucking of the column web or beam flange and web near the contact piece can occur but cannot be simulated with a two-dimensional finite element model

VALIDATION

The accuracy of the proposed numerical model was verified by means of experimental data to ensure its validity and degree of accuracy. In this section three different examples were analysed and the numerical results were compared with the corresponding experimental data.

The first example is the simply supported composite beam tested by Abdel Aziz (1986), the second example concerns the continuous composite beam tested by Ansourian (1981), while the third example deals with the composite joint tested by Kathage (1995).

Simply Supported Composite Beam

Figure 7 shows the simply supported composite beam (P14) tested to failure by Abdel Aziz (1986). The geometrical characteristics and material properties are shown in Table 3.

The finite element idealisation of the composite beam P14 is shown in Fig. 8. Due to symmetry, only half of the beam was modelled.

Figure 9 and 10 show the comparison between numerical and experimental results of composite beam P14. The load-midspan deflection curves are shown in Fig. 9, while the slip distribution along the steel-concrete interface for two load levels is plotted in Fig. 10.

The numerical results and experimental data show a good agreement not only in the elastic deformation stage but also in the plastic deformation range.

The deformed shape of composite beam P14 obtained by finite element analysis is shown in Fig. 11 and the relative slip was clearly observed at the interface between the steel beam and the concrete slab.

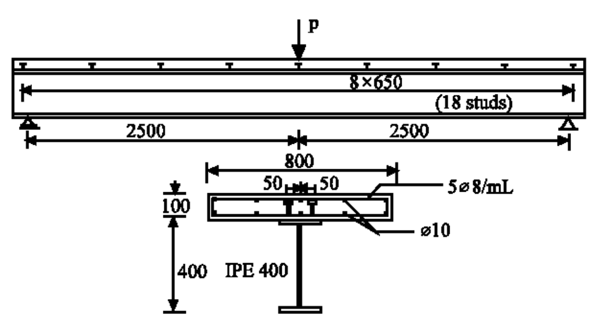

Fig. 7: Simply supported composite beam (P14)

Table 3: Geometrical characteristics and material properties for composite beam P14

Geometrical characteristics	Material properties
Concrete slab:	Cylinder compressive strength, f_{ck} = 34.7 N mm^{-2}
Thickness = 100 mm	Tensile strength, f_{ct} = 3.02 N mm^{-2}
Width = 800 mm	Young's modulus, Eq. 1, E_c = 33163 N mm^{-2}
	Poison's ratio, v_c = 0.2
	Compressive strain at maximum stress, ε_c = 0.0026
	Ultimate compressive strain, ε_{cu} = 0.0040
	Tensile strain at maximum stress, $\varepsilon_{cr} = f_{ct}/E_c$
	Ultimate tensile strain, $\varepsilon_{tu} \approx 10\ \varepsilon_{cr}$
Steel beam:	
Type of profile: IPE 400	Young's modulus E_a = 210000 N mm^{-2}, Poison's ratio, v_a = 0.3
Area = 8446 mm^2	Yield stress, f_y, Flanges: 245 N mm^{-2}, Web: 260 N mm^{-2}
Total depth = 400 mm	Ultimate stress, f_u, Flanges: 361 N mm^{-2}, Web: 372 N mm^{-2}
Flange width = 180 mm	Ultimate strain, $\varepsilon_u = 80\ \varepsilon y$, Flanges: 0.0933, Web : 0.0991
Flange thickness = 13.5 mm	Strain-hardening modulus, E_{ah}, Flanges: 1258 N mm^{-2}, Web: 1145 N mm^{-2}
Web thickness = 8.6 mm	
Reinforcing bars:	
Top area : 5 Ø 10 = 393 mm^2	Young's modulus E_s = 210000 N mm^{-2} Poison's ratio, v_s = 0.3
Bottom area : 5 Ø 10 = 393 mm^2	Yield stress, f_{sy} = 370 N mm^{-2}, Ultimate stress, f_{su} = 375 N mm^{-2}
	Ultimate strain, $\varepsilon_{su} = 25$, ε_{sy} = 0.044
	Strain-hardening modulus, E_{sh} = 118 N mm^{-2}
Stud shear connectors:	
No. of studs = 18, - Diameter×length = 19×80 mm	
Distribution of studs: uniform in 2 rows	
Connector spacing = 650 mm, Degree of shear connection = 41%	
Load-slip characteristics: Eq. 2, α = 0.8, β = 0.7 mm^{-1}	
Shear strength of connector: P_u = 130 kN, Ultimate slip capacity: S_u = 6 mm	

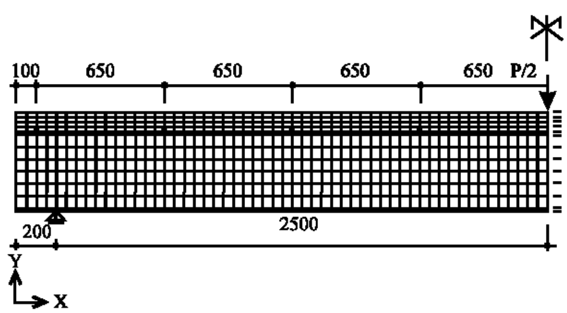

Fig. 8: Mesh and boundary condition of composite beam P14

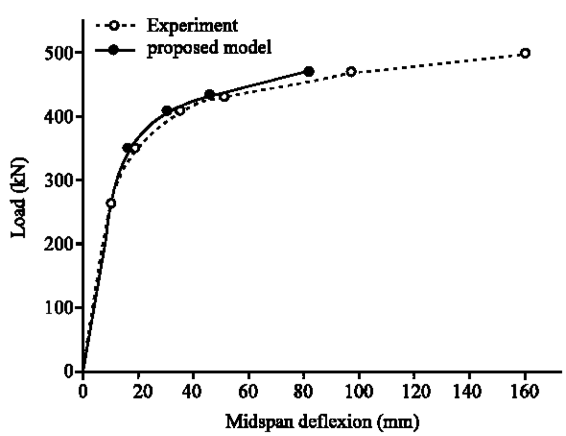

Fig. 9: Load-midspan deflection curves of composite beam P14

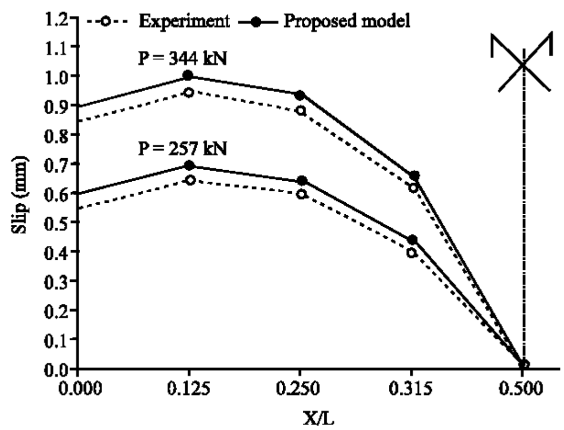

Fig. 10: Slip distribution along span at varioud load levels

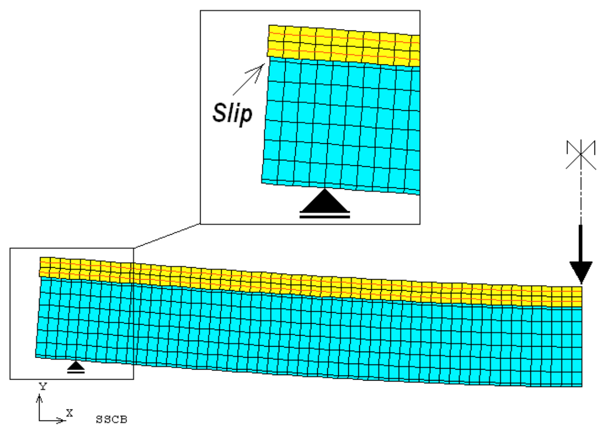

Fig. 11: Deformed shape of composite beam P14

Continuous Composite Beam

The continuous composite beam denoted CTB4 and tested by Ansourian (1981) has two equal spans of 4500 mm and is loaded symmetrically with point load at midspan. The details are reported in Fig. 12. The geometrical characteristics and material properties marked by an asterisk, such as concrete tensile strength, were not reported and have to be assumed (Table 4).

The finite element idealization of the continuous composite beam CTB4 was similar to that of the simply supported composite beam P14. However in the hogging moment regions (Zone II), the concrete slab was supposed under tension except around the front of stud shear connectors, where the concrete area is in compression. Symmetry consideration leads to the modelling of only half the continuous composite beam CTB4 as shown in Fig. 13.

The load-midspan deflection curve of the continuous composite beam CTB4 obtained from the finite element analysis was compared with corresponding experimental data in Fig. 14. A good agreement between the numerical results and experimental data is evident but the numerical curve is slightly higher than the experimental one, this is due to the slight difference between the real concrete behaviour and the material model adopted.

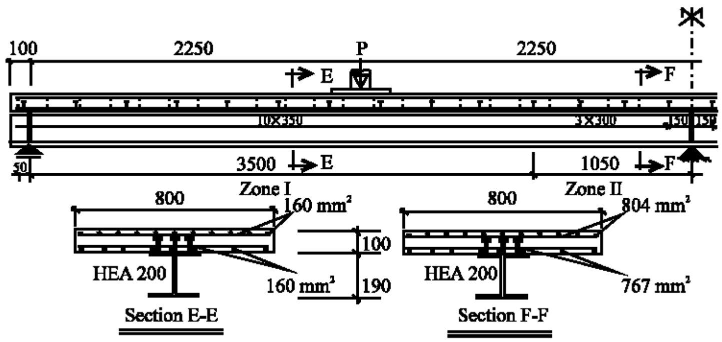

Fig. 12: Continuous composite beam (CTB4)

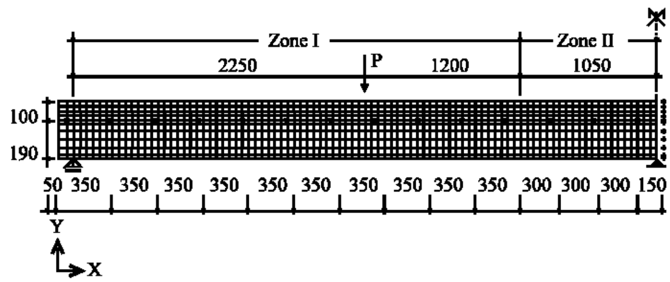

Fig. 13: Mesh and boundary conditions of continuous composite beam CTB4

Table 4: Geometrical characteristics and material properties for beam CTB4

Geometrical characteristics	Material properties
Concrete slab:	Cylinder compressive strength, $f_{ck} = 28$ N mm^{-2}
Thickness = 100 mm	Tensile strength, $f_{ct} = 2.8$* N mm^{-2}
Width = 800 mm	Young's modulus, Eq. 1, $E_c = 31331$ N mm^{-2}
Poison's ratio, $v_c = 0.2$*	
Compressive strain at maximum stress, $\varepsilon_c = 0.0025$*	
Ultimate compressive strain, $\varepsilon_{cu} = 0.0040$*	
Tensile strain at maximum stress, $\varepsilon_{cr} = f_{ct}/E_c$	
Ultimate tensile strain, $\varepsilon_{tu} \approx 10\varepsilon_{cr}$	
Steel beam:	
Type of profile: HEA 400	Young's modulus $E_a = 210000$* N mm^{-2}, Poison's ratio, $v_a = 0.3$*
Area = 5383 mm^2	Yield stress, f_y, Flanges: 236 N mm^{-2}, Web: 238 N mm^{-2}
Total depth = 190 mm	Ultimate stress, f_u, Flanges: 393 N mm^{-2}, Web: 401 N mm^{-2}
Flange width = 200 mm	Ultimate strain, ε_u, Flanges: 0.050*N mm^{-1}, Web : 0.050*
Flange thickness = 10 mm	Strain-hardening modulus, E_{ah}, Flanges: 3212* N mm^{-2}, Web: 3335* N mm^{-2}
Web thickness = 6.5 mm	
Reinforcing bars:	
+ Zone I:	
Top area = 160 mm^2	Young's modulus $E_s = 210000$* N mm^{-2} Poison's ratio, $v_s = 0.3$
Bottom area = 160 mm^2	Yield stress, $f_{sy} = 430$ N mm^{-2}, Ultimate stress, $f_{su} = 533$ N mm^{-2}
+ Zone II:	Ultimate strain, $\varepsilon_{su} = 0.0538$*
Top area = 804 mm^2	Strain-hardening modulus, $E_{sh} = 2000$* N mm^{-2}
Bottom area = 767 mm^2	
Stud shear connectors:	
No. of studs = 84, Diameter×length = 19×75 mm	
Distribution of studs: uniform in 3 rows	
Connector spacing: Zone I: 350 mm, Zone II: 300 mm	
Degree of shear connection: Zone I: 160%, Zone II: 130%	
Load-slip characteristics: (tri-linear)	
Shear strength of connector: $P_u = 11$ KN,	
Initial shear stiffness, Eq. 4, $K_{si} = 51508$* N mm^{-2}	
Elastic slip, Eq. 5, $S_e = 1.068$* mm, Plastic slip Eq. 6, $S_p = 4.27$* mm	
Ultimate slip capacity: $S_u = 7.65$* mm	

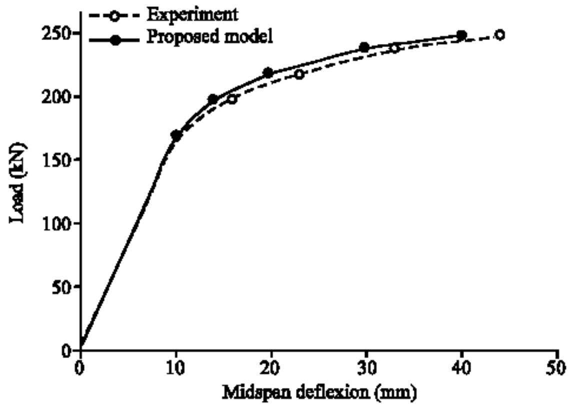

Fig. 14: Load-midspan deflection curves of continuous composite beam CTB4

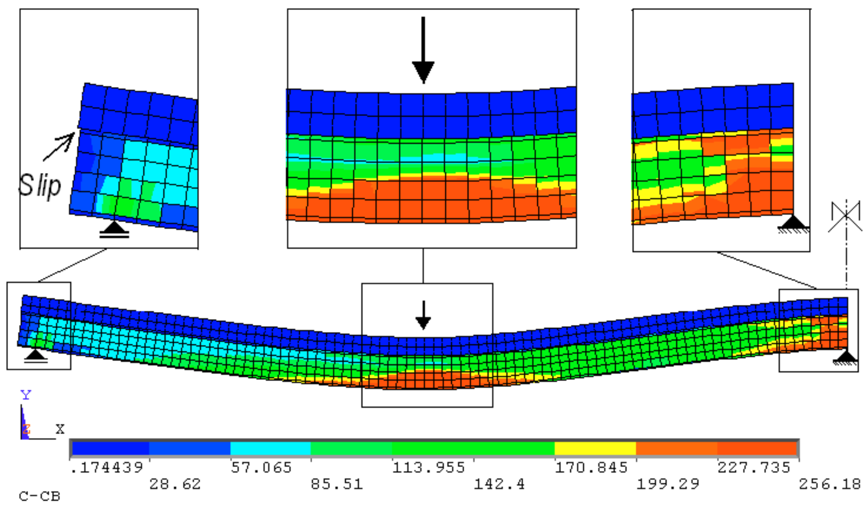

Fig. 15: Deformed shape and stress contour of continuous composite beam CTB4 at failure

Figure 15 shows the deformed shape with stress contours at failure of the continuous composite beam obtained using the finite element model. From the deformed shape, the relative slip was observed at the ends of the continuous composite beam near the external supports even with complete connection. The stress contours confirm the experimental observation that the continuous composite beam CTB4 failed firstly by cracking of the concrete slab with yielding of the reinforcing bars and yielding of the bottom steel flange over the internal support and secondly by crushing of top concrete slab and yielding of the lower part of the steel beam at midspan. It should be noted that the failure due to local bucking of continuous composite beam at the internal support can not be simulated with 2D finite element model.

Composite Joint

The description of the composite joint denoted VT2.4 and tested by Kathage (1995) is presented in Fig. 16. To simulate the internal composite joint in a braced frame, two cantilever composite beams

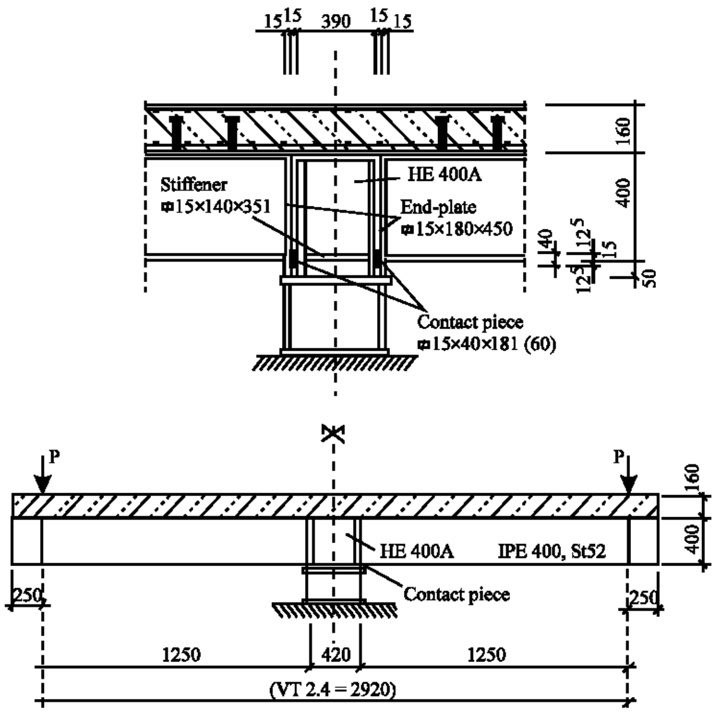

Fig. 16: Composite joint VT2.4 tested by Kathage (1995)

and one steel column were connected to form a cruciform arrangement. The steel cantilevers of an IPE 400 were attached to the column flanges with only the contact plates without any bolts. The column of an HEA400 was stiffened with transverse stiffeners welded to the web at the level of the bottom flange of the two cantilevers. Two loads of the same magnitude were applied symmetrically to each cantilever at 1.25 m from the column flange. The moment exerted on the composite joint can be easily obtained by multiplying the load with the lever arm. The rotation is calculated by measuring the horizontal displacement of the beam tension flange divided by the effective beam depth.

The geometrical characteristics and material properties of this composite joint are showed in Table 5. The values marked by an asterisk were not reported by the author; therefore they had to be assumed.

The finite element idealisation of the composite joint VT2.4 is shown in Fig. 17 noting that the material model adopted for concrete was similar to that used in hogging moment region of the continuous composite beam CTB4. Due to symmetry of the cruciform arrangement, only half of the composite joint was modelled.

The experimental (Moment-Rotation) curve for composite joint VT2.4 was compared with the corresponding numerical curve as shown in Fig. 18.

From the comparison it can be seen that the finite element model predicts very well the initial stiffness $S_{j,ini}$ and the ultimate moment M_{ju} of the composite joint. It has been observed that the experimental rotational capacity is much higher because of the brittle failure by local buckling. This instability could be explained by the high compressive stress concentration in the bottom beam flange and web near the contact piece as shown in Fig. 19. Unfortunately, this phenomenon could not be simulated by means of two-dimensional model using plan stress elements.

Table 5: Geometrical characteristics and material properties for composite joint VT2.4

Geometrical characteristics			Material properties
Concrete slab:			Cylinder compressive strength, f_{ck} = 51.3 N mm^{-2}
Thickness = 160 mm			Tensile strength, f_{ct} = 5.13* N mm^{-2}
Width = 1200 mm			Young's modulus, Eq. 1, E_c = 35048.5* N mm^{-2}
			Poison's ratio, v_c = 0.2*
			Compressive strain at maximum stress, ε_c = 0.0025*
			Ultimate compressive strain, ε_{cu} = 0.0040*
			Tensile strain at maximum stress, $\varepsilon_{cr} = f_{ct}/E_c$
			Ultimate tensile strain, $\varepsilon_{tu} \approx 10\varepsilon_{cr}$
	Steel beam	Steel column	Young's modulus E_a = 210000* N mm^{-2},
Type of profile	IPE 400	HEA 400	Poison's ratio, v_a = 0.3*
Area (mm^2)	8446	15900	Yield stress, f_y, Flanges: 424.8 N mm^{-2}, Web: 491.6 N mm^{-2}
Total depth (mm)	400	390	Ultimate stress, f_u, Flanges: 520* N mm^{-2}, Web: 586* N mm^{-2}
Flange width (mm)	180	300	Ultimate strain, ε_u, Flanges: 0.05* N mm^{-1}, Web : 0.05*
Flange thickness (mm)	13.5	19	Strain-hardening modulus, E_{ah},
Web thickness (mm)	8.6	11	Flanges: 2000* N mm^{-2}, Web: 2000* N mm^{-2}
Contact piece: 15×40×180			
End plate: 15×450×180			
Stiffener: 15×351×140			
Reinforcing bars:			Young's modulus E_s = 200000* N mm^{-2}
			Poison's ratio, v_s = 0.3
Top area = 12 Ø 12 = 1357 mm^2			Yield stress, f_{sy} = 562.1 N mm^{-2},
Bottom area =12 Ø 12 = 1357 mm^2			Ultimate stress, f_{su} = 585 N mm^{-2}
			Ultimate strain, ε_{su} = 0.05*
			Strain-hardening modulus, E_{sh} = 500* N mm^{-2}
Stud shear connectors:			
No. of studs = 12, Diameter×length = 22×120 mm			
Distribution of studs: Uniform in 2 rows			
Connector spacing: 200 mm			
Degree of shear connection: 100%			
Load-slip characteristics: (tri-linear):			
Shear strength of connector: Eq. 3, P_u = 136* KN,			
Initial shear stiffness, Eq. 4, K_{si} = 84927* N mm^{-2}			
Elastic slip, Eq. 5, S_e = 0.80* mm, Plastic slip Eq. 6, S_p = 3.20* mm			
Ultimate slip capacity: Eq. 7, S_u = 7.93* mm			

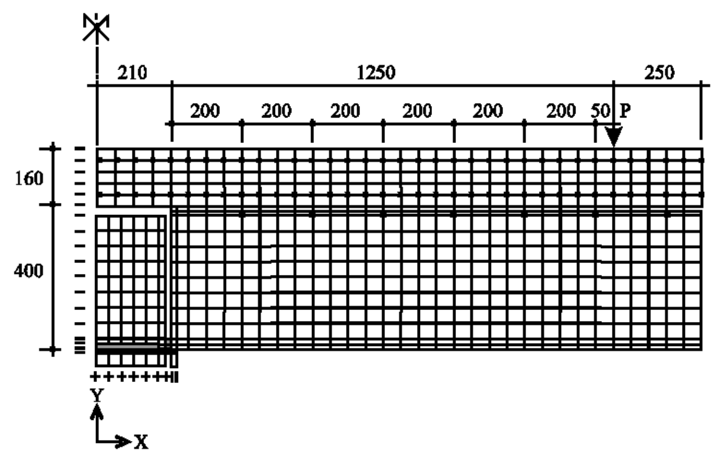

Fig. 17: Mesh and boundary conditions of composite joint VT2.4

Parametric Study

Using the finite element model which was successfully validated against experimental data, a parametric study was carried out showing the influence of the following parameters: the degree of shear

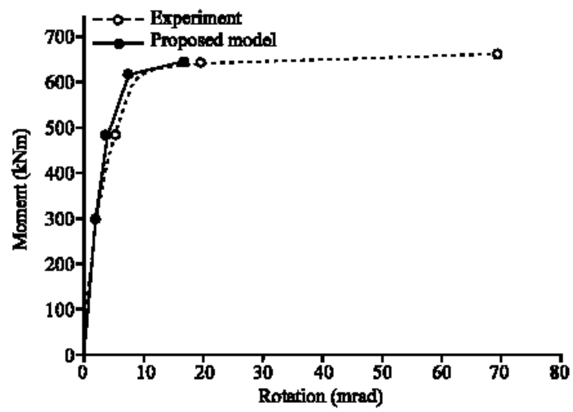

Fig. 18: Moment-rotation curves of the composite joint VT2.4

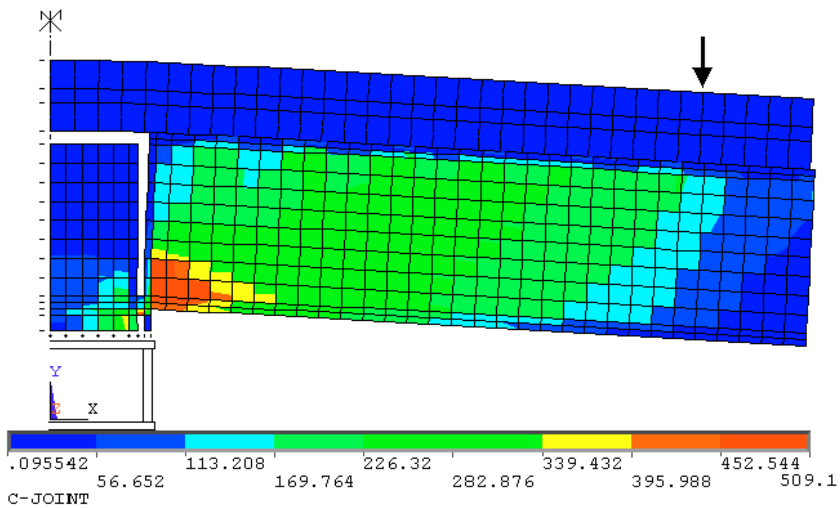

Fig. 19: Deformed shape and stress contour of the composite joint VT2.4. at M = 640 kNm

connection, the reinforcement ratio over the supports and the presence of stiffeners in the column web. The details of the parameters that had been considered are shown in Table 6, along with the geometrical characteristics and material properties of the Semi-Continuous Composite Beam system (SCCB) selected for this study and previously showed in Fig. 1. The results are relative to a point load acting on the mid-span of the composite beam.

Effect of the Degree of Shear Connection, η

The degree of shear connection was studied using four different values; 150 and 100% which indicate full shear connection and 75 and 50% representing partial shear connection in both sagging and hogging moment regions. Figure 20 shows the load-midspan deflection and load-joint rotation curves with various degrees of shear connection. The numerical results show that when the degree of shear connection decreases, the ultimate load capacity was found to decrease slightly. However, a significant increase in the midspan deflection and joint rotation was clearly observed. Figure 21 compares the load versus end-slip response for various degrees of shear connection. When the degree of shear connection

Table 6: Results of the parametric study

	SCCB	Parameters		
Same geometrical characteristics and material properties of SCCB models	SCCB model No.	Degree of shear connection (η)	Reinforcement ratio (ρ)	Presence of stiffener
Beam length: $L_b = 6000$ mm	SCCB 1	72 studs	6 Ø 12	Yes
Concrete slab:		$\eta = 150\%$		
Thickness, $h_c = 100$ mm				
Effective widths:				
$b^{+}_{eff} = 1050$ mm, $b^{-}_{eff} = 750$ mm	SCCB 2	48 studs	6 Ø 12	Yes
Compressive strength, $f_{ck} = 30$ N mm^{-2}		$\eta = 100\%$	$\rho = \frac{A_s}{A_c} = 0.9\%$	
Tensile strength, $f_{ct} = 3$ N mm^{-2}				
$E_c = 31938$ N mm^{-2}, $\nu_c = 0.2$				
Steel beam: IPE300 (S 355)	SCCB 3	36 studs	6 Ø 12	Yes
Steel column: HEA280 (S 355)		$\eta = 75\%$		
Yield stress, $f_y = 355$ N mm^{-2}				
Ultimate strain, $\varepsilon_u = 0.05$	SCCB 4	24 studs	6 Ø 12	Yes
$E = 210000$ N mm^{-2}, $\nu = 0.3$		$\eta = 50\%$		
Strain-hardening modulus, $E_h = 100$ N mm^{-2}				
Contact piece: 15×10×150 mm	SCCB 5	48 studs	4 Ø 12	Yes
Bracket: 40×35×150 mm			$A_s = 452$ mm^2	
Stiffeners: 10×24×135 mm			$\rho = \frac{A_s}{A_c} = 0.6\%$	
Reinforcing bars:				
Yield stress, $f_{sy} = 500$ N mm^{-2}				
Ultimate strain, $\varepsilon_{su} = 0.05$	SCCB 6	48 studs	8 Ø 12	Yes
$E_s = 200000$ N mm^{-2}, $\nu_s = 0.3$			$A_s = 905$ mm^2	
Strain-hardening modulus, $E_{sh} = 100$ N mm^{-2}			$\rho = \frac{A_s}{A_c} = 1.2\%$	
Stud shear connectors:				
$d = 19$ mm, $h = 80$ mm				
$P_u = 93740$ N				
$K_{si} = 45263$	SCCB 8	48 studs	6 Ø 12	No
$S_e = 1.036$ mm $S_p = 4.14$ mm $S_u = 7.58$ mm				

NB: The effectives widths $b^{\pm}_{eff}$ and the degrees of shear connection, η are designed based on the Eurocode 4 provisions

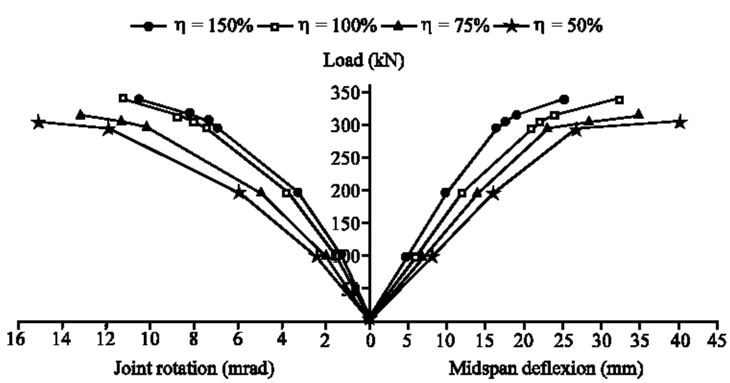

Fig. 20: Effect of the degree of shear connection, η

was reduced, the slip at the ends of the semi-continuous composite beam increased. However the rupture of the stud shear connectors did not occur in any of the four cases because the maximum slip at the ultimate load had always been less than the ultimate slip capacity of the stud shear connectors.

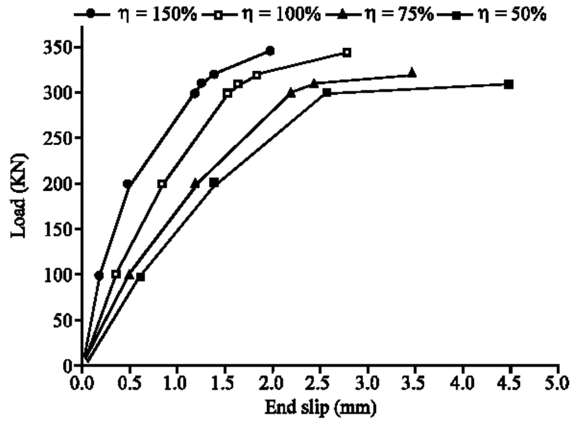

Fig. 21: Load-end-slip for various degrees of shear connection

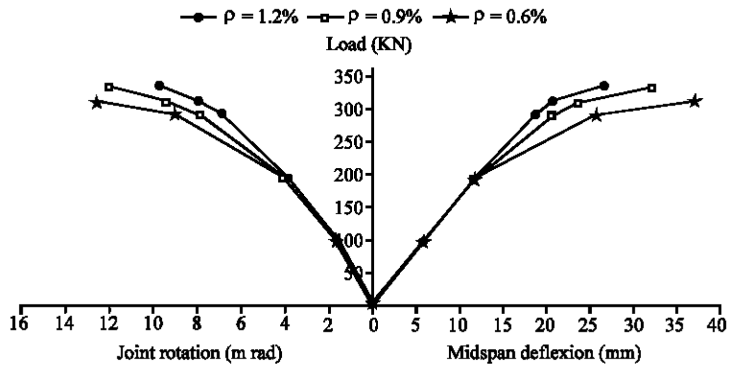

Fig. 22: Effect of the reinforcement ratio, ρ

Effect of the Reinforcement Ratio, ρ

The effect of the reinforcement ratio was also studied by varying the number of longitudinal bars over the supports. The slab reinforcement ratio for models SCCB5, SCCB2 and SCCB6 is 0.6% (small), 0.9% (medium) and 1.2% (large), respectively. From the load-midspan deflection and load-joint rotation curves shown in Fig. 22, it can be seen that an increase in the reinforcement ratio, ρ resulted in an increase of the ultimate load capacity. However, the midspan deflection and joint rotation were reduced.

Effect of the Presence of Column Web Stiffeners

The SCCB7 and SCCB2 models are similar except that the former one consists of a steel column without stiffeners. From Fig. 23, it can be observed that the presence of the stiffeners increases the ultimate load capacity and prevents the local buckling of the column web. Through the stress contours at failure of the semi-continuous composite beam SCCB7 shown in Fig. 24, the high compressive stress concentrated at the web can produce local buckling of the column web associated with excessive deformation of the column flange, leading to a premature failure in the composite joint.

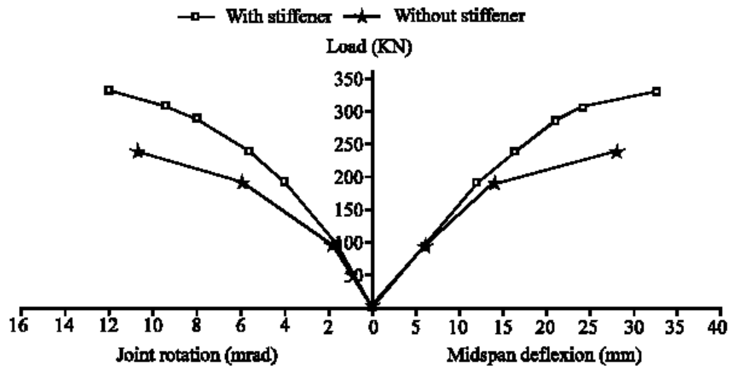

Fig. 23: Effect of the presence of column web stiffeners

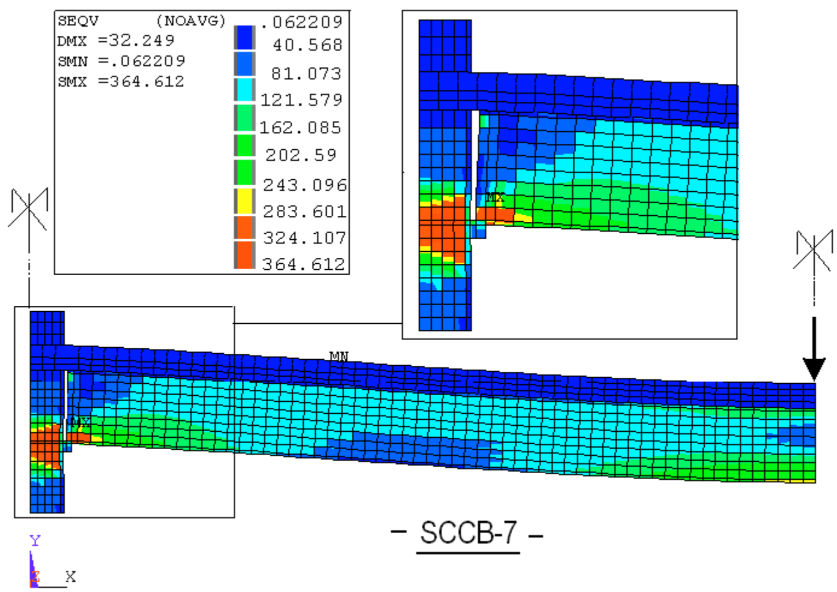

Fig. 24: Concentration of compressive stress in the unstiffened column web

CONCLUSIONS

A two-dimensional finite element model using ANSYS software has been proposed to simulate the behaviour of semi-continuous composite beams accepting the concept of partial shear connection in both sagging and hogging moment regions. The accuracy and reliability of the proposed model has been demonstrated by comparison with experimental data available in the literature. Good predictions of the midspan deflections, the joint rotations, the relative slip and the distribution of stresses and strains across the section depth have been obtained. Based on the validated model, a parametric study has been also undertaken to investigate the effects of partial shear connection, along with the effects of reinforcing ratio and the presence of column web stiffeners on the behaviour of semi-continuous composite beams. From this study it can be concluded that:

- When the degree of shear connection decreases, the ultimate load capacity has been found to decrease slightly. However, a significant increase in the midspan deflection and joint rotation has been clearly observed.
- The failure of stud shear connectors has not been observed when the degree of shear connection is partial in the sagging and hogging moment regions.
- The longitudinal reinforcing bars have made a significant contribution to develop a composite action in the beam-column joints. In addition, when the reinforcement ratio increases, the ultimate load capacity has been found to increase. However, the midspan deflection and joint rotation were reduced.
- The presence of the stiffeners increases the ultimate load capacity and prevents the local buckling of the column web.

Based on the previous results, the concept of partial shear connection in the hogging moment regions can be accepted provided that the shear connectors are sufficiently ductile. However the minimum degree of connection which can be accepted remains to be assessed.

ACKNOWLEDGMENT

The authors would like to acknowledge the support provided by the department M and S of Liège University (Belgium).

REFERENCES

Abdel Aziz, K., 1986. Numerical modeling and experimental study of composite beams with partial or spaced shear connection. Ph.D Thesis, No. D 86-3-INSA de Rennes (France).

Ansourian, P., 1981. Experiments on continuous composite beams. Proc. Inst. Civ. Eng., 2 (71): 25-51.

ANSYS, Swanson Analysis Systems. Online manual, version 10. and Theory Reference.

Aribert, J.M. and A.G. Labib, 1982. Elastoplastic calculation model of composite beams with partial connection. Revue Construction Métallique, St-Remy-lès-Chevreuse (France), 4: 3-52.

Aribert, J.M. and A.G. Lachal, 1992. Experimental investigation of composite connections and global interpretation. COST C1 Workshop in Strasbourg (France).

Aribert, J.M., E. Ragneau and H. Xu, 1993. Development of a finite element composite beam incorporating the phenomena of slip and semi-continuity with eventually local buckling. Revue Construction Métallique, St-Remy-lès-Chevreuse (France), 2: 31-49.

Bangash, M.Y.H., 1989. Concrete and Concrete Structures: Numerical Modeling and Applications. Elsevier Science Publishers Ltd., London (England).

Bascar, K., F. Shanmugam and V. Thevendran, 2002. Finite element analysis of steel-concrete composite plate girder. J. Struct. Eng. ASCE., 128 (9): 1158-1168.

Bode, H., H. Kronenberger and W. Michaeli, 1997. Composite joints-further experimental results. In: Proceedings of the International Conference on Composite Construction, Innsbruck (Austria): IABSE., pp: 433-438.

Bujnak, J. and A. Bouchair, 2005. Numerical model for steel-concrete composite beam with partial shear connection. Proceedings of Eurosteel, V.B., S.4.3, pp: 19-25.

Bursi, O.S. and R. Caldara, 1999. A non-linear finite element study of steel-concrete composite substructures with partial shear connection. J. Struct. Eng. ASCE., (Submitted).

Bursi, O.S., F.F. Sun and S. Postal, 2005. Non-linear analysis of steel-concrete composite frames with full and partial shear connection subjected to seismic loads. J. Construct. Steel Res., 61 (1): 67-92.

Diedricks, A.A., B. Uy, M.A. Bradford and D.J. Oehlers, 1999. Influence of partial shear connection on the behaviour of composite joints. 16th Australasian Conference Mechanics of structures and Materials, Sydney, pp: 303-308.

Dissanayake, U.I., I.W. Burges and J.B. Davison, 2000. Modelling of plane composite frames in unpropped construction. J. Eng. Struct., 22 (4): 283-303.

Doneaux, C., 2003. Parametric study of the behaviour of composite beams in joints to exterior columns. In: Proceedings of the 4th International Conference, STESSA, Naples (Italy), pp: 293-298.

Ebato, K., K. Morita and T. Sugiyama, 1995. Finite Element Analysis of Semi-Rigid Composite Joints. Structural Connections, Shanmugam, Choo-Pergamon (Ed.). Vol. 2. PSSC'95, 4th Pacific Structural Steel Conference, pp: 9-16.

Eurocode 4, 1992. ENV 1994-1-1. Design of composite steel and concrete structures- Part 1.1: General rules and rules of buildings. Brussels (Belgium).

Fabbrocino, G., G. Manfredi and E. Cosenza, 2002. Modelling of continuous steel-concrete composite beams: Computational aspects. J. Comput. Struct., 80 (27-30): 2241-2251.

Fu, F., D. Lam and J. Ye, 2007. Parametric study of semi-rigid composite connections with 3-D finite element approach. J. Eng. Struct., 29 (6): 888-898.

Hirst, M.J. and N.F. Yeo, 1980. The analysis of composite beams using standard finite element programs. J. Comput. Struct., 11 (3): 233-237.

Johnson, R.P. and N. Molenstra, 1991. Partial shear connection in composite beams for buildings. Proc. Inst. Civil Eng., Part 2 (91): 679-704.

Kathage, K., 1995. Contribution to the plastic calculation of hot rolled laminated beams with different types of connections. Technical Scientific Report No. 95-2, Institute of Constructional Civil Engineering, Ruhr-University of Bochum (Germany).

Kattner, M. and M. Crisinel, 2000. Finite element modelling of semi- rigid joints. J. Comput. Struct., 78 (1-3): 341-353.

Lee, S.J. and L.W. Lu, 1991. Cycle Load Analysis of Composite Connection Subassemblages. In: Connections in Steel Structures II, Bjorhovde, Colson, Hajjar, Strak (Eds.). Pitts-burgh: AISC., pp: 209-216.

Liang, Q.Q., B. Uy, M.A. Bradford and H.R. Ronagh, 2004. Ultimate strength of continuous composite beams in combined bending and shear. J. Construct. Steel Res., 60 (8): 1109-1128.

Loh, H.Y., B. Uy and M.A. Bradford, 2004. The effects of partial shear connection in the hogging moment regions of composite beams-Part I: Experimental study. J. Construct. Steel Res., 60 (6): 897-919.

Loh, H.Y., B. Uy and M.A. Bradford, 2006. The effects of partial shear connection in composite flush end plate joints- Part I: Experimental study. J. Construct. Steel Res., 62 (4): 378-390.

Nie, J.G., J.S. Fan and C.S. Cai, 2004. Stiffness and Deflection of steel-concrete composite beams under negative bending. J. Struct. Eng. ASCE., 130 (11): 1842-1851.

Oehlers, D.J. and C.G. Coughlan, 1986. The shear stiffness of stud shear connections in composite beams. J. Construct. Steel Res., 6 (4): 273-284.

Ollgaard, J.O., R.G. Slutter and J.W. Fisher, 1971. Shear strength of stud connectors in light weight and normal weight Concrete. Eng. J. AISC., 8: 55-64.

Queiroz, F.D., P.C.G.S. Vellasco and D.A. Nethercot, 2007. Finite element modelling of composite beams with full and partial shear connection. J. Construct. Steel Res., 63 (4): 505-521.

Razaqpur, A.G. and M. Nofal, 1989. A finite element for modelling the nonlinear behaviour of shear connectors in composite structures. J. Comput. Struct., 32 (1): 169-174.

Salvatore, W., O.S. Bursi and D. Lucchesi, 2005. Design, testing and analysis of high ductile partial-strength steel-concrete composite beam-to-column joints. J. Comput. Struct., 83 (28-30): 2334-2352.

Sebastian, W.M. and R.E. Mc Connel, 2000. Nonlinear FE analysis of steel- concrete composite structures. J. Struct. Eng. ASCE., 126 (6): 662-674.

Studer, M.A., 1985. Modeling of reinforced and non reinforced concrete for nonlinear calculation of beam plane structures using finite elements. International Report No. 85/2, EPFL, Lausanne (Switzerland).